International Journal of Mechanical, Industrial and Aerospace Sciences
ISSN: 2517-9950
Vol:11, No:3, 2017

# Modeling and System Identification of a Variable Excited Linear Direct Drive

Heiko Weiß, Andreas Meister, Christoph Ament, Nils Dreifke

***Abstract*—**Linear actuators are deployed in a wide range of applications. This paper presents the modeling and system identification of a variable excited linear direct drive (LDD). The LDD is designed based on linear hybrid stepper technology exhibiting the characteristic tooth structure of mover and stator. A three-phase topology provides the thrust force caused by alternating strengthening and weakening of the flux of the legs. To achieve best possible synchronous operation, the phases are commutated sinusoidal. Despite the fact that these LDDs provide high dynamics and drive forces, noise emission limits their operation in calm workspaces. To overcome this drawback an additional excitation of the magnetic circuit is introduced to LDD using additional enabling coils instead of permanent magnets. The new degree of freedom can be used to reduce force variations and related noise by varying the excitation flux that is usually generated by permanent magnets. Hence, an identified simulation model is necessary to analyze the effects of this modification. Especially the force variations must be modeled well in order to reduce them sufficiently. The model can be divided into three parts: the current dynamics, the mechanics and the force functions. These subsystems are described with differential equations or nonlinear analytic functions, respectively. Ordinary nonlinear differential equations are derived and transformed into state space representation. Experiments have been carried out on a test rig to identify the system parameters of the complete model. Static and dynamic simulation based optimizations are utilized for identification. The results are verified in time and frequency domain. Finally, the identified model provides a basis for later design of control strategies to reduce existing force variations.

***Keywords*—**Force variations, linear direct drive, modeling and system identification, variable excitation flux.

## I. Introduction

LDDs are actuators to carry out diverse moving applications. The deployment of LDDs is increasing since several years due to their advantageous properties. These include high stiffness, great dynamic actuation and precise positioning capabilities. The lack of a rotational-translational transducer means less wear and thus cost savings during the operating time. Because the vertical attraction force is much larger than the horizontal driving force, the bearings must be designed according to mechanic requirements. A well-suited solution in terms of stiffness and low friction is air bearings.

The examined linear drive is a three-phase hybrid stepper motor with air bearings working on the principle of Sawyer [1]. The function principle is based on the alternating strengthening and weakening of the phases' legs and is outlined well in [2]. Energizing the phases' sinusoidal yields smoother operation compared to block commutation. Deployed as positioning system, the LDD requires sophisticated hardware and control algorithms. A side effect of the motor principle is the occurrence of force variations affecting the smoothness of operation as well as the positioning accuracy. Their reasons are force ripple and cogging forces. Force ripple is arisen by non-sinusoidal force functions due to production tolerances, inhomogeneous magnet fields or non-synchronism of commutation. Cogging is a typical property of motors based on Sawyer's principle. Since the magnetic field tends to minimize the reluctance of the magnetic circuit, attractive forces arise that are responsible for cogging.

Methods to reduce the effects of force variations can be divided into constructive and control based techniques. Constructive methods comprise geometric modifications and variations of the magnetic circuit. These include skewing of magnets, the groove geometry, or yoke variations exemplary shown in [3]. A novel structure of a pure linear stepper motor was presented in [4] with the purpose of minimizing the cogging forces of the passive phases. One group of control based techniques is aimed to compensate the disturbing force ripple by feedforwarding. The feedforward implies a position dependent force ripple function that is added to the control signal. For estimating the force ripple, observers [5] or adaptive structures [6] are applied. Another category of control based methods comprises modified commutation laws. These are obtained by optimization problems yielding non-sinusoidal commutation [7] and field orientated commutation [8].

The main issue of this contribution is the modeling and identification process of a variable excited LDD. In order to design advanced controllers and techniques for noise reduction, it is necessary to work with a nonlinear model. In [9], a finite element (FE) model structure of a phase module is built up. With it, a nonlinear but static force characteristic is obtained and mapped as look-up table. For comparison, a reluctance network was examined as well. Both approaches need a high number of parameters that can restrict the identifiability. Parameter identification is a big challenge for nonlinear systems and depends on the choice of the model structure. To apply methods of linear system identification,

H. Weiß is with the Institute for Automation and Systems Engineering, Ilmenau University of Technology, 98684, P.O Box 100565, Germany (phone: 03677 69 1467, e-mail: heiko.weiss@tu-ilmenau.de).

A. Meister is with the Institute of Process Measurement and Sensor Technology, Ilmenau University of Technology, 98684 Germany (e-mail: andreas.meister@tu-ilmenau.de).

C. Ament is head of the Chair for Control Engineering, University of Augsburg, 86159, Germany (e-mail: christoph.ament@informatik.uni-augsburg.de).

N. Dreifke is executive director of Pasim Direktantriebe GmbH®, 98529 Suhl, Germany (e-mail: n.dreifke@direktantriebe.de).

Volterra type equations [10] and neural networks [11] are used. However, these approaches imply a high number of parameters to achieve sufficiently good results.

In this contribution, a new innovative constructive design of an LDD aiming to reduce force variations is shown in Section II. Subsequently, the experimental setup is presented. For the new design a system model is required to test and optimize control strategies. The mathematical model composed of nonlinear ordinary differential equations (ODEs) is presented in Section IV. To identify the model, subsystems are considered and identified experimentally with static and simulation based dynamic optimization. Afterwards, the identified complete model is validated in Section V.

## II. Novel Motor Design

In order to reduce force variations and the connected noise, a new design of an LDD as shown in Fig. 1 is examined. The stator is made of iron and has the characteristic tooth structure like the mover. That is built by three-phase modules separated by magnetic insulating spacers. Each phase module has a thrust coil wound through both legs of the iron yoke. Perpendicular to it the enabling coil is placed between the legs. The direction of the middle phase coils alternates to avoid interactions of the magnetic circuits. To comply with the functional principle, the phase modules are shifted by one third of the tooth period to each other. The central idea of the novel design is switching off the enabling coils when no thrust force is needed. Therefore, all of them are excited synchronously, whereas the thrust coils are commutated commonly with three sinusoidal currents that are shifted one third period to each other.

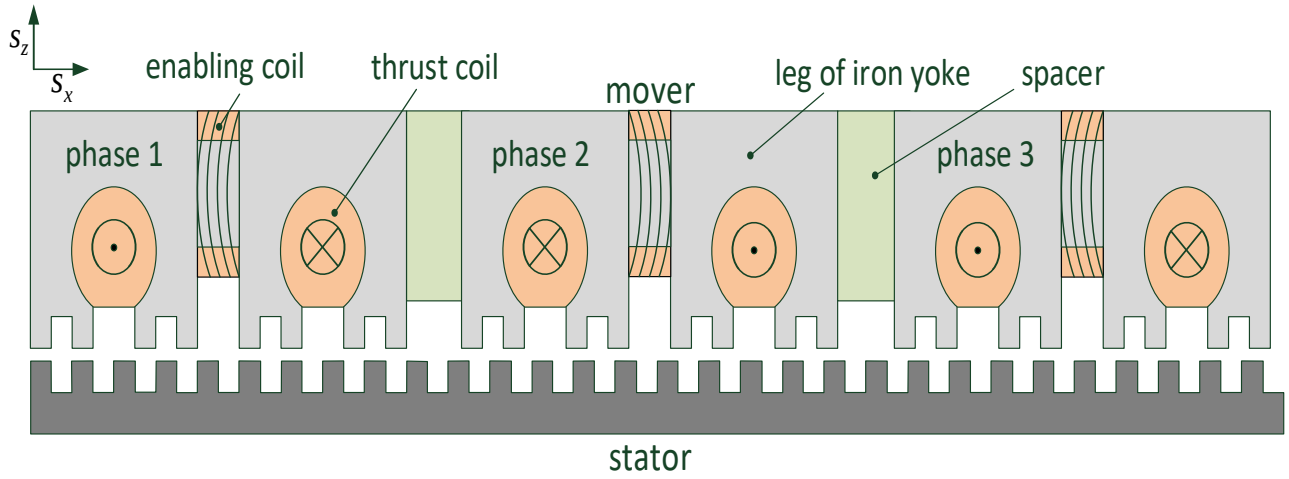


Fig. 1 Topology of the coil-excited three-phase LDD developed by Pasim Direktantriebe GmbH®

## III. Experimental Setup

The experimental setup (see Fig. 2) provides the base for identification and later research of the new design. The core of the setup is the LDD placed on a massive frame. Besides the LDD, the test rig consists of power electronics, sensor devices and real time hardware. The LDD itself has a guide carriage moving along the linear axis. On the guide carriage, the mover module is fixed with a spring sheet. To ensure high stiffness of the mover bearing, especially when the enabling coils are energized less, there are sloping surfaces on the sides of the stator. In addition to the air bearing of the mover, two air bearings on the top and two on each side of the stator exist. Thus, a downforce is created by sloping air bearings avoiding the mover hovering away. The compressed air is supplied by a mobile compressor. An aluminum adapter plate provides the mountings for a three-axis accelerometer and the spring sheet linking the mover with the guide carriage. The accelerometer is made of piezoelectric material providing a high dynamic bandwidth. Furthermore, a capacitive distance sensor is deployed to measure the vibration displacement of the mover. As metal target object of the cylindrical probe, the adapter plate is utilized. Both sensor devices include amplifiers to adjust the measuring range and condition the sensor signals for the real time hardware. Besides the data acquisition the real time hardware is responsible for calculation and output of the currents for the coil systems. Control algorithms and processes like initialization run are carried out with a sample rate of 10 kHz. Linear analog amplifiers transduce the commanded voltage signals into appropriate currents for both coil systems. Each phase coil is energized by two amplifiers generating a maximum current of 6 A together. Hence, 12 amplifiers are deployed at all providing a sufficiently high source of electrical energy.

## IV. Modeling and System Identification

Modeling and parameter identification are conducted with theoretical basic equations that are augmented with methods of experimental system identification. During the modeling process, it was taken into account that system nonlinearities were described with regard to simple identification and control design. Since a nonlinear model is supposed to be created, the system must be excited in a wide span with not only one

operating point combining the input and state values diversely. Furthermore, it must be considered that the system is examined in a sufficiently high frequency range.

The parameter identification is commonly based on the objective to minimize the sum of least squares with respect to boundaries.

$$\begin{aligned} &\underset{\underline{p}}{\mathrm{Min}} \sum_{i=1}^{N} \left( y - f(\underline{p}, \underline{u}) \right)^2 \\ &s.t. \quad \underline{p}_{\min} < \underline{p} < \underline{p}_{\max} \end{aligned} \tag{1}$$

Hereby, $y$ notes the measured values, $N$ the number of samples and $f$ the modeled function that is dependent on the input $\underline{u}$ and parameter vector $\underline{p}$. Since a pattern search algorithm [12] is applied parameter linearity of $f$ is not crucial. The static approach (1) is suitable for parameters with dedicated experiments where input and output data can be measured. Model parts not corresponding with these requirements must be identified otherwise. Hence, a dynamic optimization is carried out whereby several subsystems can be included into optimization regarding the transient behavior of the system model. But the unseparated influence of different parameter sets implies the presence of a pareto optimum. The formulation of the dynamic optimization problem for a MIMO-system reads as follows:

$$\begin{aligned} &\underset{\underline{p}}{\mathrm{Min}} \sum_{i=1}^{N} \left( \underline{y} - \underline{h}(\underline{x}, \underline{p}, \underline{u}) \right)^2 \\ &s.t. \quad \underline{p}_{\min} < \underline{p} < \underline{p}_{\max} \\ &\qquad \dot{\underline{x}} = \underline{f}(\underline{x}, \underline{p}, \underline{u}) \end{aligned} \tag{2}$$

Here $\underline{f}$ describes the ODE and $\underline{h}$ the output equations of the state space model. The derivatives of the states are numerically integrated and available in every time step. The strategy is to apply (1) if possible or to provide an initial parameter set for (2) respectively in order to reduce the computing time. Nevertheless, for special experiments a subdivision of the outputs (e.g. horizontal and vertical position) can decrease the number of parameters which is beneficial for the optimization process, too. As stated before, the complete system is divided into several subsystems. These are presented in the next subsections.

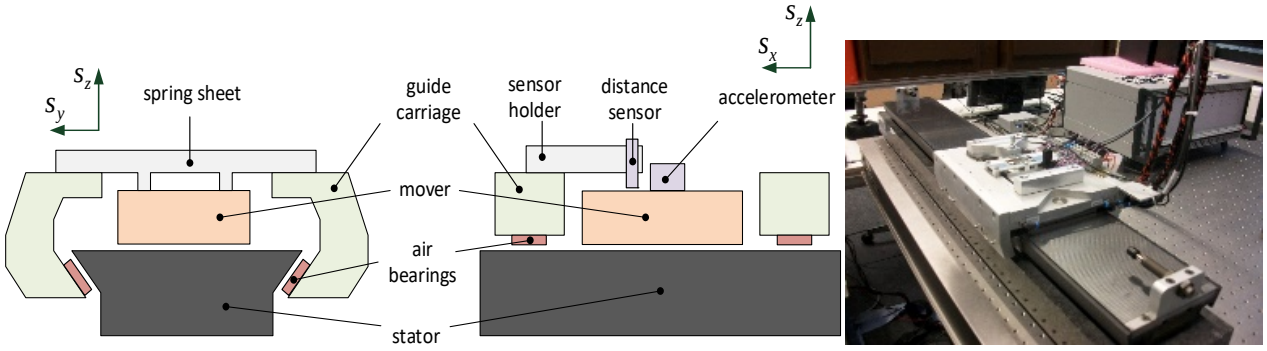


(a) (b) (c)

Fig. 2 Experimental setup; schematic cutaway of front (a) and side view (b) and test rig (c). The linear drive is located on a massive table with a breadboard

*A. Current Dynamics*

The current dynamics includes the behavior of the electric circuit containing power electronics and coil systems. On the assumption that all phases have equal characteristic behavior, the three phases can be modeled as one electrical circuit. The linear analog amplifier is mapped as ideal current source with the control current $I$. A series of resistance $R$ and inductance $L$ completes the circuit. Position dependent inductance and other magnetic dynamic effects are implied to the force functions, that will be discussed later. Hence, the electric circuit of each coil system is depicted as a $PT_1$-element

$$\frac{i}{I} = \frac{1}{s \cdot \tau + 1} \tag{3}$$

with the time constant $\tau$ and the desired current $I$ of the circuit resulting in the ODE

$$I = i + \tau \cdot \frac{di}{dt} \tag{4}$$

for each coil system. To identify the time constants, the mover is fixed at one position to comply with the model assumptions. As exciting signals, a chirp and a sequence of white noise having a sufficient frequency range are applied. According to (3), the basis for identification is a parametric $PT_1$-structure. Using the measurement data of the input $I$ and output $i$ the time constants are estimated. For comparison, a non-parametric spectral model is created additionally. The resulting frequency responses are shown in Fig. 3. Both the $PT_1$ and the frequency model have a similar edge frequency of approximately 1 kHz. The enabling coils (Fig. 3 (b)) exhibit a slightly higher frequency working range.

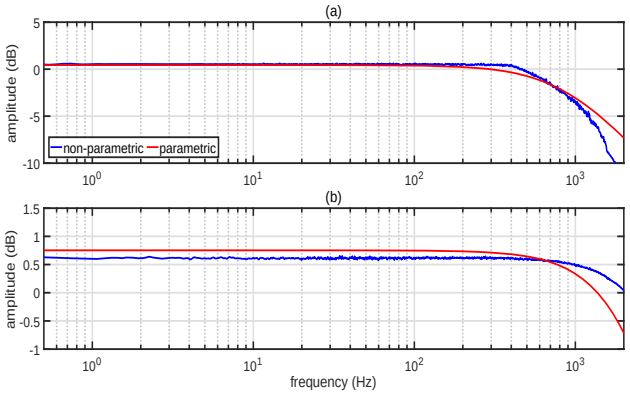


Fig. 3 Amplitude frequency responses of the thrust coils (a) and the enabling coils (b)

### *B. Mechanic Subsystem*

The mechanic subsystem can be divided into horizontal and vertical dynamics. The horizontal dynamics describes the positioning movement of the armature overlaid with vibrations. In vertical direction, force fluctuations are noticeable, too. Nevertheless, the vibrations of the mover occur in random mode shapes, that cannot be captured with a simple model structure.

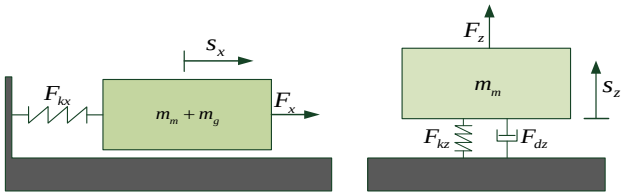


Fig. 4 Model for horizontal and vertical dynamics of the LDD

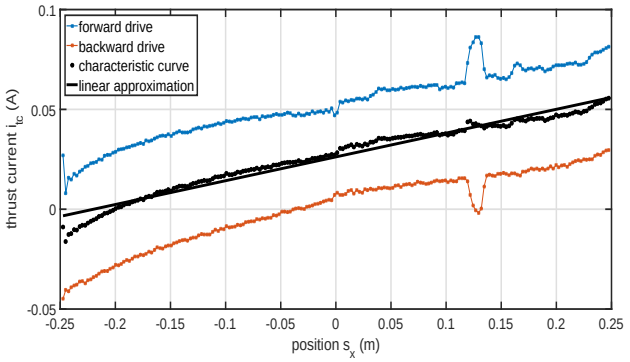


Fig. 5 Identification of the horizontal stiffness, caused by light unevenness of the stator surfaces

A model approach for horizontal and vertical dynamics is sketched in Fig. 4. In order to reduce model complexity, simplifications are made. Among others, this concerns the neglection of elasticity of the stator and frame. Furthermore, examinations of the vertical stiffness, modeling the air bearings, reveal a dominant stiffness between guide carriage and stator. Hence, it is described as fixed coupling. The remaining linkages of the spring sheet and the air bearing to the mover can be combined to one stiffness. Considering the simplifications, the equation for the horizontal movements results in

$$(m_g + m_m) \cdot \ddot{s}_x + F_{kx} = F_x \tag{5}$$

The force $F_x$ has to overcome the mass inertia of the mover $m_m$ and the guide carriage $m_g$. Due to slightly inclined stator surfaces the streaming air produces a horizontal force additionally. Measurements have proven that this effect can be modeled as horizontal stiffness $F_{kx}$. The characteristic curve was obtained by driving the whole movement range slowly forward and backward for eliminating disturbances as especially seen on position 0.13 m. The resulting curve (see Fig. 5) was approximated with a linear function

$$F_{kx} = k_{x0} + k_{x1} \cdot s_x \tag{6}$$

The mechanic friction is not modeled explicitly but included in unmagnetization terms of the force function (see section C).

The vertical movement characterized by vibrations can be stated as

$$m_m \cdot \ddot{s}_z + F_g + F_{kz} + F_{dz} = F_z \tag{7}$$

with a gravitational force component $F_g$, the vertical stiffness $F_{kz}$ and damping force $F_{dz}$. The characteristic curve of the vertical stiffness is achieved by loading the mover with different weights and measuring the according displacement with the distance sensor. Therefore, a linear approach is chosen as well as for the damping force, that is identified simulation based according to approach (2).

### *C. Force Functions*

#### 1. Horizontal

Force functions are applied to model the nonlinear effects resulting from simplifications made in current dynamics, the neglection of the magnetic domain, and the periodic appearance of force variations. The force function for x-direction is composed of three components:

$$F_x = F_{stat,x} + F_{fv,x} - F_{uml,fr,x} \tag{8}$$

The static term $F_{stat,x}$ generates the thrust force which is overlaid with velocity dependent force variations $F_{fv,x}$ and unmagnetization and friction losses $F_{uml,fr,x}$. The static term

$$F_{stat,x} = \left[ f_{sigm}(i_{tc}) + f_{pol}(i_{tc}) \right] \cdot \left[ f_{sigm}(i_{ec}) + f_{pol}(i_{ec}) \right] \cdot f_{sigm,dead}(i_{ec}) \tag{9}$$

depends on the thrust current $i_{tc}$ and enabling current $i_{ec}$.

Therefore, a sigmoid function modeling the saturation effects and a polynomial to refine the approximation are used. To map the dead zone of the enabling current an additional

sigmoid is deployed suppressing the force action up to 0.8 A. For identification, the two-dimensional input domain is varied and the force is measured with a spring scale. The result of the static optimization according to (2) is the characteristic curve shown in Fig. 6 representing (9).

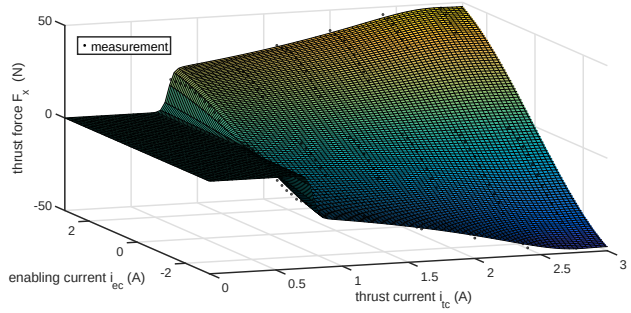


Fig. 6 Characteristic curve of the static force component with dead zone due to enabling current

The force variation

$$F_{fv,x} = f_{fv}(s_x) \cdot g_{fv}(i_{tc}, i_{ec}, \dot{s}_x) \tag{10}$$

includes a position dependent mode shape $f_{fv}$ that is weighted with $g_{fv}$. The latter depends on both input currents and velocity. The vibration is assumed as a trigonometric function that generally can be expressed with parameters for amplitude, frequency and phase:

$$f_{fv}(s_x) = \sum_{i=1}^{m} a_{i1} \cdot \sin(a_{i2} \cdot s_x + a_{i3}) \tag{11}$$

During experiments, an invariant behavior of the vibration mode was detected revealing not only quantitative but also qualitative changes that are especially effected by velocity. Thus, an upper velocity operation range beyond 0.5 m/s is applied to identify the mode shapes represented by two trigonometric functions. The evaluation function

$$g_{fv} = f_{tc}(i_{tc}) \cdot f_{ec}(i_{ec}) \cdot f_v(v_x) \tag{12}$$

is modeled with polynomial functions as general approach and tanh respecting the saturation of the input current action. Each dependent variable is described with a separate function. Hereby, simulation based optimization is applied considering all parameters of (12).

The third component of the force function $F_{uml,fr,x}$ represents the combination of unmagnetization and friction losses (UML). The UML contain iron losses caused by transforming the direction of the Weiß' domains and eddy current losses. Eddy currents arise from induced voltage in the iron yoke. Mechanical friction is not caused by body contact but from drag. The drag for its part is composed of form drag and skin friction. Skin friction occurs from the interaction of air bearings and stator surface, whereas form drag is determined by the outer geometry of the armature. Due to the frictional character of UML, equivalent model approaches can be used as presented in [2], [13], and thus, a whole parameter set can be neglected. When creating the model, it was taken into account that the equations are differentiable. Thus, the common concepts with signum terms are excluded. As approach, a nonlinear static friction model presented in [14] is applied:

$$\begin{aligned} F_{uml,fr,x} = {} & \zeta_1 \cdot \tanh(\zeta_2 \cdot v_x) + \zeta_3 \cdot v_x \\ & + \zeta_4 \cdot \left[ \tanh(\zeta_5 \cdot v_x) - \tanh(\zeta_6 \cdot v_x) \right] \end{aligned} \tag{13}$$

The equation is inspired by Stribeck methodology including static friction, viscous friction, and their transition.

2. Vertical

Considering the vertical force, there is no need for an explicit term of UML and friction since it can be included into force variations. The reason is that static force and force variations work in the same vertical displacement range opposite to horizontal case. The overall vertical force reads

$$F_z = F_{stat,z} + F_{fv,z} \tag{14}$$

The static force $F_{stat,z}$ is identified by exciting the enabling coils stepwise and measuring the displacement. By means of the vertical stiffness curve, an equivalent static force can be estimated related to the set current. This relation is approximated well with a sigmoid function characterized by three design parameters:

$$F_{stat,z} = p_{z1} \cdot \left[ 1 + \tanh\left( \frac{p_{z2} \cdot i_{ec} - p_{z3}}{2} \right) \right] \tag{15}$$

The thrust current is not considered since if one leg flux is increased, the other one is decreased synchronously by the same amount. Additionally, there is a negative measurement side-effect caused by leaving the resting position of armature with activated thrust current.

The vertical force variations $F_{fv,z}$ are designed identically to the horizontal ones. The process of identification contains a static optimization for initialization followed by a dynamic simulative optimization. Since the system mode shapes are invariant and not in phase with the simulation, a new variable must be created to realize an optimization process. This modified value describes the strength of the vibrations as sum of the last 250 (corresponds to 25 ms) absolute values:

$$v_{z,mean} = \sum_{k}^{k+250} \left| v_z(k) \right| \tag{16}$$

The curves presented in Fig. 7 demonstrate a sufficient identification result of force variations. Fig. 7 (a) shows the progress of the real vertical velocity, and Fig. 7 (b) shows the newly introduced variable of (16) used for optimization.

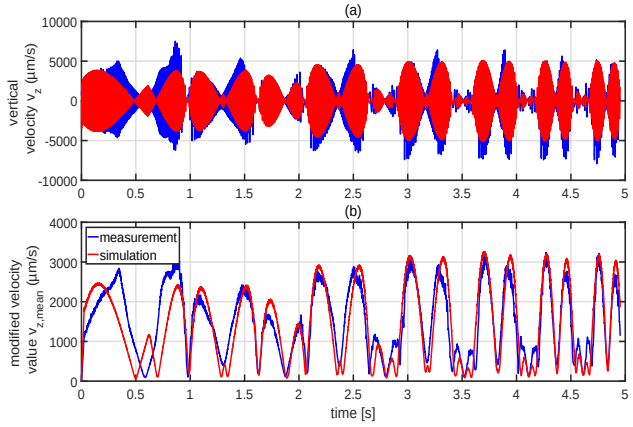


Fig. 7 Vertical force variations presented by vertical velocity (a) and modified vertical velocity value (b)

Since all model components are described and identified, the complete model is available. After all, there is an ODE-system composed of (4) for both coil systems on the electric side and the mechanical subsystem for horizontal (5) an vertical (7) dynamics. The differential equations a transformed into a six-degree state space yielding th nonlinear form

$$\dot{\underline{x}} = \underline{f}(\underline{x},\underline{u})$$
$$\underline{y} = \underline{h}(\underline{x},\underline{u}) \qquad (1$$

with input vector u, state space vector x and output vector y:

$$u = \left[ I_{tc} \quad I_{ec} \right]^T$$
$$x = \left[ i_{tc} \quad i_{ec} \quad s_x \quad \dot{s}_x \quad s_z \quad \dot{s}_z \right]^T \qquad (1$$
$$y = \left[ s_x \quad s_z \right]^T$$

## V. Validation

To ensure validity of the identified MIMO model, additional experiments are carried out. Thereby, the real system as well as the model are excited with the same input currents. In Fig. 8, the comparison of both the simulation model and real system is presented in time-domain. The thrust current is alternating rectangularly from minus to plus 1 A, whereas the enabling coils are applied with a chirp added to a 2 A offset. The position $s_x$ exhibits a small divergence after the first period of the chirp. The trend to move in negative direction is caused by the horizontal stiffness. This drift is overlaid with fluctuations of movement direction that result from the alternating thrust current. The vertical vibrations $s_z$ can only be modeled qualitatively due to their invariant structure. When moving over the stator, they arise as position dependent vibrations. Another effect is fluctuations of attractive force caused by the chirp excitation of the enabling current. Due to the strong nonlinear character of the system, it is hard to achieve a quantitative correspondence in the whole operation range. But, the model exhibits a good qualitative behavior that is most important for control design, so that a wide diversity of input signals can be applied.

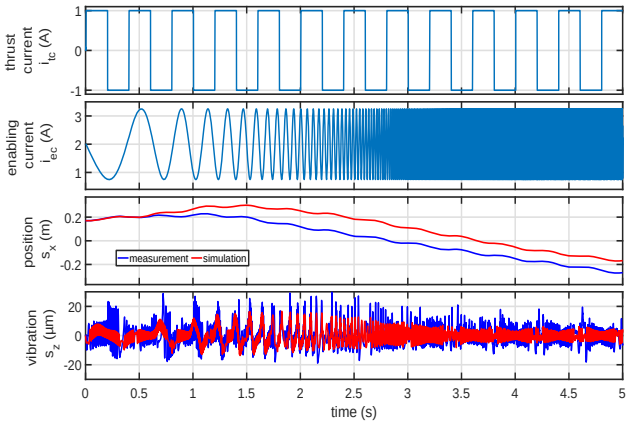


Fig. 8 System and model responses on dynamic excitation of the inputs

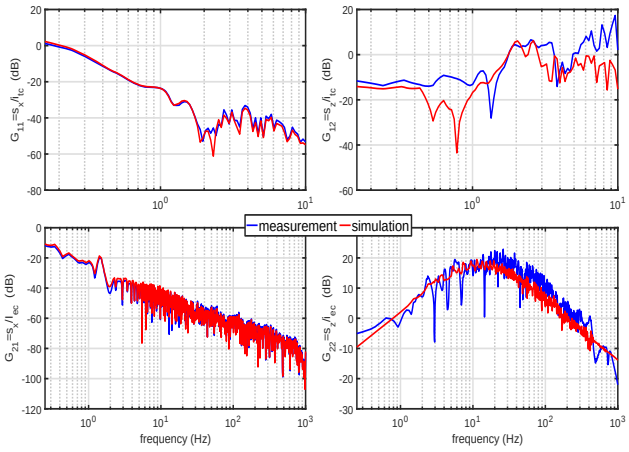


Fig. 9 Transfer functions of the MIMO system model

To examine the dynamic behavior, the frequency domain is investigated. Hence, a linearization of input-output behavior must be taken into account. A correlation analysis as it was applied to the current dynamics is carried out. The result is presented as frequency response matrix in Fig. 9. This matrix depicts the dynamic effect of the thrust current $i_{tc}$ (first row) and enabling current $i_{ec}$ (second row) to the movement $s_x$ (first column) and vertical vibrations $s_z$ (second column). $G_{11}$ reveals the typical behavior of a delay element with decreasing amplitude. In $G_{12}$, an anti-resonant spot arises caused by mutual compensation of mode vibrations and input excitations. Generally, the influence of the enabling coils on the x-movement is low and has a constant decrease along the frequency range due to mass inertia of the armature. $G_{22}$ comprises the effect of the enabling coils on the vertical vibrations. The increase at lower frequency is determined by the high-pass filter of the displacement that is utilized to eliminate steady components. A decrease in higher frequency ranges means that the effect of the enabling current is low.

## VI. Conclusion

In this contribution, a novel design of a LDD based on hybrid stepper technology is presented and modeled. The modeling and identification process are goal-oriented minimizing the number of equations and parameters while maintaining reasonable quality of the identified model. Bypassing the magnetic domain reduces the number of equations and parameters further. The coil systems are modeled as delay elements. The mechanic behavior is divided into horizontal and vertical dynamics in which nonlinear force functions are included. In order to identify the model, the subsystems are examined individually. As identification approaches, a static optimization is utilized for characteristic curves. Furthermore, a simulation based dynamic optimization is applied to identify parameter sets of nonlinear functions regarding the model outputs. The identified subsystems are presented achieving good results. The resulting complete system is validated and matches the behavior of the test rig very well. Thus, a base to apply control strategies to reduce force variations and the connected noise is available.

## Acknowledgment

The authors would like to acknowledge the support of the German Ministry of Economics and Energy (BMWi) within the ZIM cooperation project (FKZ: KF2250120WD4).

## References

[1] H.-D. Stölting, E. Kallenbach, W. Amrhein, Handbuch Elektrische Kleinmaschinen, Hanser, 2011.
[2] A. E. Quaid, Y. Xu, R.L. Hollis, “Force characterization and commutation of planar linear motors, IEEE ICRA Proceedings, Albuquerque, 1997.
[3] P. Joerges, W. Schinköthe, “Geometrical optimized cogging forces at linear direct drives”, 8.ETG/GMM-Fachtagung Innovative Klein- und Mikroantriebstechnik, Würzburg, 2010.
[4] S. Lorand, I.A. Viorel, I. Chisu, Z. Kovacs, “A Novel Double Salient Permanent Magnet Linear Motor”, Proceedings of the International Conference on Power Electronics, Drives and Motion (PCIM), Nürnberg, 1999, vol. Intelligent Motion, pp. 285-290.
[5] J. Malaizé, J. Lévine, “An Observer-Based Design for Cogging Forces Cancellation in Permanent Magnet Linear Motors”, Joint 48th IEEE Conference on Decision and Control and 28th Chinese Control Conference, Shanghai, 2009.
[6] H.-S. Ahn, Y.Q. Chen, H. Dou, “State-Periodic Adaptive Compensation of Cogging and Coulomb Friction in Permanent-Magnet Linear Motors”, IEEE Transactions on Magnetics, Vol. 41, No. 1, 2005.
[7] C. Röhrig, A. Jochheim, “Identification and Compensation of Force Ripple in Linear Permanent Magnet Motors”, Proceedings of the American Control Conference, Arlington, 2001.
[8] Y.W. Zhu, K.S. Jung, J.H. Cho, “The Reduction of Force Ripples of PMLSM Using Field Oriented Control Method”, CES/IEEE 5th International Power Electronics and Motion Control Conference, Shanghai, 2006.
[9] R. Wislati, H. Haase, “Using COMSOL Multiphysics for the Modelling of a Hybrid Linear Stepper Motor”, Proceedings of the COMSOL Users Conference, Grenoble, 2007.
[10] T. Treichl, S. Hofmann, D. Schröder, „Identification of Nonlinear Dynamic Systems with Multiple Inputs and Single Output using discrete-time Volterra Type Equations”, Proceedings of 15th International Symposium on Mathematical Theory of Networks and Systems, Notre Dame, Indiana, 2002.
[11] S. Beineke, H. Wertz, F. Schütte, H. Grotstollen, N. Fröhleke, “Identification of Nonlinear Two-Mass Systems for Self-Commissioning Speed Control of Electrical Drives”, Proceedings of the 24th Annual Conference of the IEEE, Industrial Electronics Society, Aachen, 1998.
[12] C. Audet, J. E. Dennis Jr., "Analysis of Generalized Pattern Searches.", SIAM Journal on Optimization, Volume 13, Number 3, 2003, pp. 889–903.
[13] F. Henrotte, K. Hameyer, “A Dynamical Vector Hysteresis Model Based on an Energy Approach”, IEEE Transactions on Magnetics, Vol. 42, pp. 899-902, 2006.
[14] C. Makkar, W.E. Dixon, W.G. Sawyer, G. Hu, “A New Continuously Differentiable Friction Model for Control Systems Design”, Proceedings of the 2005 IEEE/ASMEInternational Conference on Advanced Intelligent Mechatronics, Monterey, California, 2005.